Journal of Applied Analysis and Computation
Volume 13, Number 4, August 2023, 1837–1851
Website:http://www.jaac-online.com
DOI:10.11948/20220258

A TWO-GRID DECOUPLED FINITE ELEMENT METHOD FOR THE STATIONARY CLOSED-LOOP GEOTHERMAL SYSTEM*

Haochen Liu[1] and Pengzhan Huang[1,†]

Abstract A two-grid decoupled finite element method is proposed and analyzed for the stationary closed-loop geothermal model, which is coupled by the Navier-Stokes/Darcy equations and the heat equations with some interface conditions. The main idea of the proposed method is to solve the nonlinear problem on a coarse grid to obtain an initial approximation, then solve the decoupled, linear problem on a fine grid. Hence, the original problem is solved by two subsystems using the two-grid technique, which will save computational time. Moreover, the stability of the proposed method is proved, and numerical examples are presented.

Keywords Closed-loop geothermal model, finite element method, two-grid algorithm, decoupled strategy.

MSC(2010) 65N30, 35Q35.

1. Introduction

This paper addresses the numerical simulation of the closed-loop geothermal system, which consists of a main geothermal reservoir and several closed-loop heat exchange pipes. The governing equations of this system include two parts: the Boussinesq equations describe fluid flow in the pipelines, and the Darcy equations and the heat equation govern fluid flow in the porous media of the geothermal reservoir. Besides, two flows are coupled through heat exchanging conditions and no-fluid communication conditions on the interface. Hence, this problem is complicated to deal with in numerical simulation because of its interface conditions and coupling of multiple physical quantities. In fact, the system not only contains the velocity and the pressure but also includes the temperature field in both fluid subdomains.

In [21], a decoupled stabilized finite element approach is proposed for an unsteady closed-loop geothermal system. As a matter of fact, the decoupling method has become a popular method for solving such a hybrid model, making existing single-model solvers locally applicable and saving much computational cost. In this paper, based on the decoupled strategy, we will design the two-grid method for solving the considered model. Some details of the two-grid method can be

†The corresponding author.
Email: liuhaochen@stu.xju.edu.cn(H. Liu), hpzh@xju.edu.cn(P. Huang)
[1]College of Mathematics and System Sciences, Xinjiang University, Urumqi 830017, China
*The authors were supported by the Natural Science Foundation of Xinjiang Province (No. 2021D01E11) and the Natural Science Foundation of China (No. 11861067).

found in the works of Xu [24, 25], which is further investigated and applied to the Burger's equation [8], the Navier-Stokes equations [12,13,18], the natural convection system [9, 10, 27], the Stokes-Darcy model [22], the magnetohydrodynamics equations [23], the Navier-Stokes/Darcy equations [3,5], and other problems [11,14–17]. However, to the authors' knowledge, no paper is mentioned on the two-grid method for the stationary closed-loop geothermal model.

2. The stationary closed-loop geothermal model

Consider a bounded domain $\Omega \subset \mathbb{R}^d$ ($d = 2$ or 3)which consists of two subdomains Ω_f and Ω_p with Lipschitz continuous boundaries $\partial\Omega_f$ and $\partial\Omega_p$, separated by the interface Γ. The vectors n_f and n_p are the unit normal vectors that point outward from the fluid layer Ω_f and porous media layer Ω_p, respectively. The unit outward normal vectors satisfy the condition of $n_p = -n_f$ on the interface Γ. Now, we consider the stationary closed-loop geothermal model on the whole domain as follows.

In Ω_f, the fluid flow with heat transfer is governed by the Navier-Stokes equations coupled with the heat equation for the velocity u_f, pressure p_f and temperature θ_f [26]

$$
\begin{aligned}
&-\nu\Delta u_f + (u_f \cdot \nabla)\, u_f + \nabla p_f = \nu^2 Gr\theta_f e && \text{in } \Omega_f, && (2.1)\\
&\nabla \cdot u_f = 0 && \text{in } \Omega_f, && (2.2)\\
&-\kappa_f \Delta\theta_f + u_f \cdot \nabla\theta_f = g_f && \text{in } \Omega_f. && (2.3)
\end{aligned}
$$

In Ω_p, the fluid in the porous media is described by the Darcy equations coupled with the heat equation for the velocity u_p, pressure p_p and temperature θ_p [26]

$$
\begin{aligned}
&\frac{\nu}{Da} u_p + \nabla p_p = \nu^2 Gr\theta_p e && \text{in } \Omega_p, && (2.4)\\
&\nabla \cdot u_p = 0 && \text{in } \Omega_p, && (2.5)\\
&-\kappa_p \Delta\theta_p + u_p \cdot \nabla\theta_p = g_p && \text{in } \Omega_p, && (2.6)
\end{aligned}
$$

where ν, Gr are the kinetic viscosity and Grashof number, respectively. Besides, the vector e represents a unit vector in the direction of gravitational acceleration. Da is the Darcy number of the porous media, which is assumed to be isotropic and homogeneous. Further, κ_i and g_i, $i = f, p$, refer to the thermal conductivity of fluid and the heat sources, respectively. Here $i = f$ denotes the function in Ω_f and $i = p$ means the function in Ω_p.

Besides, the system (2.1)-(2.6) is considered in conjunction with the following boundary conditions on $\partial\Omega_f$ and $\partial\Omega_p$

$$
\begin{aligned}
&u_f = 0 \ \text{ on } \partial\Omega_f\backslash\Gamma, \quad \theta_f = 0 \ \text{ on } \Gamma_{fD}, \quad \frac{\partial\theta_f}{\partial n_f} = 0 \ \text{ on } \Gamma_{fN},\\
&u_p \cdot n_p = 0 \ \text{ on } \partial\Omega_p\backslash\Gamma, \quad \theta_p = 0 \ \text{ on } \Gamma_{pD}, \quad \frac{\partial\theta_p}{\partial n_p} = 0 \ \text{ on } \Gamma_{pN},
\end{aligned}
$$

where Γ_{fD} and Γ_{fN} are the pipe region boundaries with $\partial\Omega_f\backslash\Gamma = \Gamma_{fN} \cup \Gamma_{fD}$ and denote the Dirichlet and Neumann boundary conditions, respectively, and Γ_{pD} and Γ_{pN} are the porous media region boundaries with $\partial\Omega_p\backslash\Gamma = \Gamma_{pN} \cup \Gamma_{pD}$ and denote the Dirichlet and Neumann boundary conditions, respectively.

Furthermore, for the closed-loop geothermal system, in order to describe heat exchanging and no-fluid communication on the interface Γ, we utilize several critical interface conditions as follows [21]:

$$u_p \cdot n_p = 0, \quad u_f \cdot n_f = 0, \quad \text{(No-communication conditions)}; \tag{2.7}$$

$$\theta_f = \theta_p, \quad \text{(Continuity of temperature)}; \tag{2.8}$$

$$\kappa_f \frac{\partial \theta_f}{\partial n_f} + \kappa_p \frac{\partial \theta_p}{\partial n_p} = 0, \quad \text{(Continuity of heat flux)}; \tag{2.9}$$

$$u_f \cdot \tau = 0, \quad \text{(No-slip condition)}, \tag{2.10}$$

where τ is the unit tangential vector along Γ.

Next, we need to introduce some notations and function spaces to establish a variational formulation of the stationary closed-loop geothermal model. Firstly, for $1 \le q \le \infty$ and $m \in \mathbb{N}^+$, we denote the Lebesgue space by $L^q(\Omega)$ and the Sobolev space by $H^m(\Omega)$ [1]. Secondly, we denote the inner product and norm on $L^2(\Omega)^d$ by $(\cdot,\cdot)$ and $\|\cdot\|_0$, respectively. We also denote the norm $\|\cdot\|_m$ of the Sobolev space $H^m(\Omega)$ $(m \ge 1)$. Finally, we define the following function spaces:

$$X_f := \left\{ v_f \in H^1(\Omega_f)^d : v_f = 0 \text{ on } \partial\Omega_f \backslash \Gamma \right\},$$

$$X_p := \left\{ v_p \in L^2(\Omega_p)^d, \nabla \cdot v_p \in L^2(\Omega_p) : v_p \cdot n_p = 0 \text{ on } \partial\Omega_p \backslash \Gamma \right\},$$

$$Y_f := \left\{ q_f \in L^2(\Omega_f) : (q_f, 1) = 0 \right\}, \quad Y_p := \left\{ q_p \in L^2(\Omega_p) : (q_p, 1) = 0 \right\},$$

$$W_f := \left\{ \omega_f \in H^1(\Omega_f) : \omega_f = 0 \text{ on } \Gamma_{fD} \right\}, \quad W_p := \left\{ \omega_p \in H^1(\Omega_p) : \omega_p = 0 \text{ on } \Gamma_{pD} \right\}.$$

Besides, we define some product spaces

$$X := X_f \times X_p, \quad Y := Y_f \times Y_p, \quad W := W_f \times W_p,$$

and

$$W_\Gamma := \left\{ \boldsymbol{\omega} = (\omega_f, \omega_p) \in W_f \times W_p : \omega_f|_\Gamma = \omega_p|_\Gamma \right\}.$$

Moreover, we list the Poincaré inequality [1] as follows. For $u_f \in X_f$, we have

$$\|u_f\|_0 \le C_p \|\nabla u_f\|_0,$$

where C_p is a constant which depends only on Ω.

Now, we show the variational formulation of the considered couple model: find $(\boldsymbol{u}, \boldsymbol{p}, \boldsymbol{\theta}) \in X \times Y \times W$ such that for any $(\boldsymbol{v}, \boldsymbol{q}, \boldsymbol{\omega}) \in X \times Y \times W_\Gamma$:

$$a(\boldsymbol{u}, \boldsymbol{v}) - b(\boldsymbol{v}, \boldsymbol{p}) + c_f(u_f; u_f, v_f) = \nu^2 Gr\,(\boldsymbol{\theta} e, \boldsymbol{v}), \tag{2.11}$$

$$b(\boldsymbol{u}, \boldsymbol{q}) = 0, \tag{2.12}$$

$$\bar{a}(\boldsymbol{\theta}, \boldsymbol{\omega}) + \bar{c}(\boldsymbol{u}; \boldsymbol{\theta}, \boldsymbol{\omega}) - \bar{a}_\Gamma(\theta_f, [\boldsymbol{\omega}]) + \bar{a}_\gamma([\boldsymbol{\theta}], [\boldsymbol{\omega}]) = (\boldsymbol{g}, \boldsymbol{\omega}), \tag{2.13}$$

where

$$a(\boldsymbol{u}, \boldsymbol{v}) = a_f(u_f, v_f) + a_p(u_p, v_p), \quad b(\boldsymbol{v}, \boldsymbol{p}) = b_f(v_f, p_f) + b_p(v_p, p_p),$$

$$c_f(u_f; u_f, v_f) = ((u_f \cdot \nabla) u_f, v_f), \quad (\boldsymbol{\theta} e, \boldsymbol{v}) = (\theta_f e, v_f) + (\theta_p e, v_p),$$

$$\bar{a}(\boldsymbol{\theta}, \boldsymbol{\omega}) = \bar{a}_f(\theta_f, \omega_f) + \bar{a}_p(\theta_p, \omega_p), \quad \bar{c}(\boldsymbol{u}; \boldsymbol{\theta}, \boldsymbol{\omega}) = \bar{c}_f(u_f; \theta_f, \omega_f) + \bar{c}_p(u_p; \theta_p, \omega_p),$$

$$\bar{a}_\Gamma(\theta_f, [\boldsymbol{\omega}]) = \kappa_f \int_\Gamma \nabla \theta_f \cdot n_f \cdot (\omega_f - \omega_p), \quad \bar{a}_\gamma([\boldsymbol{\theta}], [\boldsymbol{\omega}]) = \frac{\kappa_f \gamma}{\widetilde{h}} \int_\Gamma (\theta_f - \theta_p)(\omega_f - \omega_p).$$

Here $\widetilde{h}>0$ is the mesh size which will be defined in the next section, $\gamma>0$ is the stabilized parameter which is independent of $\widetilde{h}$, $[\boldsymbol{\theta}]=\theta_f-\theta_p$ and

$$a_f(u_f,v_f)=\nu(\nabla u_f,\nabla v_f),\quad a_p(u_p,v_p)=\frac{\nu}{Da}(u_p,v_p),\quad b_f(v_f,p_f)=(p_f,\nabla\cdot v_f),$$
$$b_p(v_p,p_p)=(p_p,\nabla\cdot v_p),\quad \bar{a}_f(\theta_f,\omega_f)=\kappa_f(\nabla\theta_f,\nabla\omega_f),\quad \bar{a}_p(\theta_p,\omega_p)=\kappa_p(\nabla\theta_p,\nabla\omega_p),$$
$$\bar{c}_f(u_f;\theta_f,\omega_f)=(u_f\cdot\nabla\theta_f,\omega_f),\quad \bar{c}_p(u_p;\theta_p,\omega_p)=(u_p\cdot\nabla\theta_p,\omega_p).$$

Remark 2.1. Note that the interface terms in (2.13) appear due to the dissipative character of Nitsche's coupling. Unlike the penalty methods, they are consistent with the original differential equations but ensure the stability of the finite element method. More details are discussed in [6,21].

Lemma 2.1 ([4,27]). *The trilinear forms $c_f(\cdot;\cdot,\cdot)$ and $\bar{c}_i(\cdot;\cdot,\cdot)$, $i=f$ or p satisfy:*

(i) In view of $H^1(\Omega)\hookrightarrow L^4(\Omega)$, we have

$$|c_f(u_f;v_f,w_f)|\le N\|\nabla u_f\|_0\|\nabla v_f\|_0\|\nabla w_f\|_0,\quad \forall u_f,v_f,w_f\in X_f,$$
$$|\bar{c}_f(u_f;\theta_f,\omega_f)|\le \bar{N}\|\nabla u_f\|_0\|\nabla\theta_f\|_0\|\nabla\omega_f\|_0,\quad \forall u_f\in X_f,\theta_f,\omega_f\in W_f,$$
$$|\bar{c}_p(u_p;\theta_p,\omega_p)|\le \bar{N}\|u_p\|_1\|\nabla\theta_f\|_0\|\nabla\omega_p\|_0,\quad \forall u_p\in X_p,\theta_p,\omega_p\in W_p,$$

where $N,\bar{N}$ are the constants depending only on Ω;

(ii) Under the condition of $\nabla\cdot u_i=0$, there hold that

$$c_f(u_f;v_f,v_f)=0\ \forall\, u_f,v_f\in X_f;\quad \bar{c}_i(u_i;\theta_i,\theta_i)=0\ \forall\, u_i\in X_i,\ \theta_i\in W_i.$$

3. Two-grid decoupled finite element method

We consider the regular triangulation $\tau_{\widetilde{h}}(\Omega)=\{T\}$ of Ω with mesh size $\widetilde{h}$ ($\widetilde{h}=h$ or H with $h\ll H$) whose value is the diameter $\widetilde{h}_T$ of the element T. We assume that the triangulations $\tau_{\widetilde{h}}(\Omega_f)$ and $\tau_{\widetilde{h}}(\Omega_p)$ induced on the sub-domains Ω_f and Ω_p are compatible on the interface Γ.

Set $X_{\widetilde{h}}\times Y_{\widetilde{h}}\times W_{\widetilde{h}}\subset X\times Y\times W$ be three finite element spaces. The spaces $X_{f\widetilde{h}}$ and $Y_{f\widetilde{h}}$ are chosen to satisfy the so-called LBB condition, such as MINI element. In particular, the $X_{p\widetilde{h}}\times Y_{p\widetilde{h}}$ can be chosen as Raviart-Thomas element. In the whole domain Ω for the temperatures, we choose linear Lagrangian element. Hence, the finite element discretization applied to the problem (2.11)-(2.13) leads to a coupled discrete problem as follows: find $\left(\boldsymbol{u}_{\widetilde{h}},\boldsymbol{p}_{\widetilde{h}},\boldsymbol{\theta}_{\widetilde{h}}\right)\in X_{\widetilde{h}}\times Y_{\widetilde{h}}\times W_{\widetilde{h}}$ such that for any $\left(\boldsymbol{v}_{\widetilde{h}},\boldsymbol{q}_{\widetilde{h}},\boldsymbol{\omega}_{\widetilde{h}}\right)\in X_{\widetilde{h}}\times Y_{\widetilde{h}}\times W_{\widetilde{h}}$

$$a(\boldsymbol{u}_{\widetilde{h}},\boldsymbol{v}_{\widetilde{h}})-b(\boldsymbol{v}_{\widetilde{h}},\boldsymbol{p}_{\widetilde{h}})+c_f(u_{f,\widetilde{h}};u_{f,\widetilde{h}},v_{f,\widetilde{h}})=\nu^2Gr\left(\boldsymbol{\theta}_{\widetilde{h}}e,\boldsymbol{v}_{\widetilde{h}}\right),\tag{3.1}$$
$$b(\boldsymbol{u}_{\widetilde{h}},\boldsymbol{q}_{\widetilde{h}})=0,\tag{3.2}$$
$$\bar{a}(\boldsymbol{\theta}_{\widetilde{h}},\boldsymbol{\omega}_{\widetilde{h}})+\bar{c}(\boldsymbol{u}_{\widetilde{h}};\boldsymbol{\theta}_{\widetilde{h}},\boldsymbol{\omega}_{\widetilde{h}})-\bar{a}_\Gamma(\theta_{f,\widetilde{h}},[\boldsymbol{\omega}_{\widetilde{\boldsymbol{h}}}])+\bar{a}_\gamma([\boldsymbol{\theta}_{\widetilde{h}}],[\boldsymbol{\omega}_{\widetilde{h}}])=\left(\boldsymbol{g},\boldsymbol{\omega}_{\widetilde{\boldsymbol{h}}}\right).\tag{3.3}$$

Now, we recall the local inverse inequality [21]. For $\theta_{\widetilde{h}}\in W_{\widetilde{h}}$, there exists a constant C_{in}, which depends only on the minimum angles of $T_{\widetilde{h}}$, such that

$$\left\|\theta_{\widetilde{h}}\right\|_\Gamma\le C_{in}^{1/2}\widetilde{h}^{-1/2}\left\|\theta_{\widetilde{h}}\right\|_0,\tag{3.4}$$

where $\|\cdot\|_\Gamma=\|\cdot\|_{L^2(\Gamma)}$.

The following theorem shows the stability of the discrete problem (3.1)-(3.3).

Theorem 3.1. *Let $(\boldsymbol{u}_{\widetilde{h}}, \boldsymbol{p}_{\widetilde{h}}, \boldsymbol{\theta}_{\widetilde{h}}) \in X_{\widetilde{h}} \times Y_{\widetilde{h}} \times W_{\widetilde{h}}$ be a solution of the finite element scheme (3.1)-(3.3). Assume the functions g_p, $g_f \in L^2(\Omega)$. If γ satisfies the condition $\gamma \gg C_{in}$, then we have the stability of the finite element discretization system*

$$\left\|\nabla\theta_{f,\widetilde{h}}\right\|_0^2 + \left\|\nabla\theta_{p,\widetilde{h}}\right\|_0^2 \leq \eta^2, \tag{3.5}$$

$$\left\|\nabla u_{f,\widetilde{h}}\right\|_0^2 + \frac{1}{Da}\left\|u_{p,\widetilde{h}}\right\|_0^2 \leq (\nu\xi\eta)^2, \tag{3.6}$$

where $\xi = C_p Gr \max\{C_p, \sqrt{Da}\}$ and $\eta = \frac{C_p}{\min\{\kappa_f,\kappa_p\}}\|\boldsymbol{g}\|_0$.

Proof. First, choosing $\boldsymbol{\omega}_{\widetilde{h}} = \boldsymbol{\theta}_{\widetilde{h}}$ in (3.3) and using Lemma 2.1 get

$$\begin{aligned}&\bar{a}_f\left(\theta_{f,\widetilde{h}}, \theta_{f,\widetilde{h}}\right) + \bar{a}_p\left(\theta_{p,\widetilde{h}}, \theta_{p,\widetilde{h}}\right) + \frac{\kappa_f\gamma}{\widetilde{h}}\int_\Gamma(\theta_{f,\widetilde{h}} - \theta_{p,\widetilde{h}})(\theta_{f,\widetilde{h}} - \theta_{p,\widetilde{h}})\\ =&\kappa_f\int_\Gamma \nabla\theta_{f,\widetilde{h}}\cdot n_f\cdot(\theta_{f,\widetilde{h}} - \theta_{p,\widetilde{h}}) + (g_f, \theta_{f,\widetilde{h}}) + \left(g_p, \theta_{p,\widetilde{h}}\right).\end{aligned} \tag{3.7}$$

Thanks to the Cauchy-Schwarz inequality, Young inequality, and local inverse inequality (3.4), we obtain

$$\begin{aligned}&\kappa_f\left\|\nabla\theta_{f,\widetilde{h}}\right\|_0^2 + \kappa_p\left\|\nabla\theta_{p,\widetilde{h}}\right\|_0^2 + \frac{\kappa_f\gamma}{\widetilde{h}}\left\|\theta_{f,\widetilde{h}} - \theta_{p,\widetilde{h}}\right\|_\Gamma^2\\ \leq&\frac{\kappa_f C_{in}}{2\gamma}\left\|\nabla\theta_{f,\widetilde{h}}\right\|_0^2 + \frac{\kappa_f\gamma}{2\widetilde{h}}\left\|\theta_{f,\widetilde{h}} - \theta_{p,\widetilde{h}}\right\|_\Gamma^2\\ &+\frac{\kappa_f}{2}\left\|\nabla\theta_{f,\widetilde{h}}\right\|_0^2 + \frac{\kappa_p}{2}\left\|\nabla\theta_{p,\widetilde{h}}\right\|_0^2 + \frac{C_p^2}{2\min\{\kappa_f,\kappa_p\}}\|\boldsymbol{g}\|_0^2,\end{aligned}$$

which leads to

$$\kappa_f(1-\frac{C_{in}}{\gamma})\left\|\nabla\theta_{f,\widetilde{h}}\right\|_0^2 + \kappa_p\left\|\nabla\theta_{p,\widetilde{h}}\right\|_0^2 + \frac{\kappa_f\gamma}{\widetilde{h}}\left\|\theta_{f,\widetilde{h}} - \theta_{p,\widetilde{h}}\right\|_\Gamma^2 \leq \frac{C_p^2}{\min\{\kappa_f,\kappa_p\}}\|\boldsymbol{g}\|_0^2. \tag{3.8}$$

Hence, if the stabilized parameter $\gamma \gg C_{in}$, then one finds

$$\left\|\nabla\theta_{f,\widetilde{h}}\right\|_0^2 + \left\|\nabla\theta_{p,\widetilde{h}}\right\|_0^2 \leq \eta^2, \tag{3.9}$$

where $\eta = \frac{C_p}{\min\{\kappa_f,\kappa_p\}}\|\boldsymbol{g}\|_0$.

Second, set $\boldsymbol{v}_{\widetilde{h}} = \boldsymbol{u}_{\widetilde{h}}$, $\boldsymbol{q}_{\widetilde{h}} = \boldsymbol{p}_{\widetilde{h}}$ in (3.1), (3.2), respectively.

$$a_f(u_{f,\widetilde{h}}, u_{f,\widetilde{h}}) + a_p(u_{p,\widetilde{h}}, u_{p,\widetilde{h}}) = \nu^2 Gr\left(\theta_{f,\widetilde{h}}e, u_{f,\widetilde{h}}\right) + \nu^2 Gr\left(\theta_{p,\widetilde{h}}e, u_{p,\widetilde{h}}\right). \tag{3.10}$$

By using the Cauchy-Schwarz inequality, Poincaré inequality, and Young's inequality, we obtain

$$\begin{aligned}\nu\left\|\nabla u_{f,\widetilde{h}}\right\|_0^2 + \frac{\nu}{Da}\left\|u_{p,\widetilde{h}}\right\|_0^2 \leq&C_p^2\nu^3\frac{C_p^2Gr^2}{2}\left\|\nabla\theta_{f,\widetilde{h}}\right\|_0^2 + \frac{\nu}{2}\left\|\nabla\vec{u}_{f,\widetilde{h}}\right\|_0^2\\ &+C_p^2\nu^3\frac{DaGr^2}{2}\left\|\nabla\theta_{p,\widetilde{h}}\right\|_0^2 + \frac{\nu}{2Da}\left\|\vec{u}_{p,\widetilde{h}}\right\|_0^2.\end{aligned} \tag{3.11}$$

Hence, combining (3.11) with (3.9), we have the following result

$$\left\|\nabla u_{f,\widetilde{h}}\right\|_0^2+\frac{1}{Da}\left\|u_{p,\widetilde{h}}\right\|_0^2\leq C_p^2\nu^2\max\left\{C_p^2Gr^2,DaGr^2\right\}\eta^2. \tag{3.12}$$

□

To obtain the error estimates, we assume that there exist $R_{\widetilde{h}}:X\to X_{\widetilde{h}}$, $Q_{\widetilde{h}}:Y\to Y_{\widetilde{h}}$ and $P_{\widetilde{h}}:W\to W_{\widetilde{h}}$ such that (see [26]): for all $\boldsymbol{v}\in X\cap(H^2(\Omega_f)^d\times H^1(\Omega_p)^d)$, $\boldsymbol{q}\in Y\cap H^1(\Omega)$, and $\boldsymbol{\omega}\in W\cap H^2(\Omega)$

$$\begin{aligned}&\|\nabla(v_f-R_{\widetilde{h}}v_f)\|_0+\left\|v_p-R_{\widetilde{h}}v_p\right\|_0\leq C\widetilde{h}(\|v_f\|_2+\|v_p\|_1),\\&\|\boldsymbol{q}-Q_{\widetilde{h}}\boldsymbol{q}\|_0+\|\nabla(\boldsymbol{\omega}-P_{\widetilde{h}}\boldsymbol{\omega})\|_0\leq C\widetilde{h}(\|\boldsymbol{q}\|_1+\|\boldsymbol{\omega}\|_2).\end{aligned} \tag{3.13}$$

Then, we consider the following error estimates for (3.1)-(3.3). For convenience, we separate the errors into two parts,

$$\begin{aligned}&u_i-u_{i,\widetilde{h}}=u_i-R_{\widetilde{h}}u_i+R_{\widetilde{h}}u_i-u_{i,\widetilde{h}}:=\chi_i+\psi_i,\ i=f\text{ or }p.\\&p_i-p_{i,\widetilde{h}}=p_i-Q_{\widetilde{h}}p_i+Q_{\widetilde{h}}p_i-p_{i,\widetilde{h}}:=\rho_i+\pi_i,\ i=f\text{ or }p.\\&\theta_i-\theta_{i,\widetilde{h}}=\theta_i-P_{\widetilde{h}}\theta_i+P_{\widetilde{h}}\theta_i-\theta_{i,\widetilde{h}}:=\phi_i+\varphi_i,\ i=f\text{ or }p.\end{aligned}$$

Theorem 3.2. *Under the assumption of Theorem 3.1, suppose that the following conditions hold*

$$\begin{aligned}&\frac{\nu}{2}-N\nu\xi\eta-Gr^2C_p^2\nu^3\max\{\frac{3C_p^2}{2\kappa_f},\frac{Da}{\kappa_p}\}\varpi_f>0,\\&\frac{\nu}{2Da}-Gr^2C_p^2\nu^3\max\{\frac{3C_p^2}{2\kappa_f},\frac{Da}{\kappa_p}\}\varpi_p>0,\end{aligned} \tag{3.14}$$

where $\varpi_f=4\bar{N}^2\kappa_f^{-1}\|\nabla\theta_f\|_0^2$, $\varpi_p=4\bar{N}^2\kappa_p^{-1}\|\theta_p\|_2^2$. *Let* $(\boldsymbol{u},\boldsymbol{p},\boldsymbol{\theta})$ *be the solution of coupled model* (2.11)-(2.13) *and* $(\boldsymbol{u}_{\widetilde{h}},\boldsymbol{p}_{\widetilde{h}},\boldsymbol{\theta}_{\widetilde{h}})$ *be the finite element solution of* (3.1)-(3.3). *Then, we have the following error estimate:*

$$\|\nabla(u_f-u_{f,\widetilde{h}})\|_0+\|u_p-u_{p,\widetilde{h}}\|_0+\|\boldsymbol{p}-\boldsymbol{p}_{\widetilde{h}}\|_0+\|\nabla(\boldsymbol{\theta}-\boldsymbol{\theta}_{\widetilde{h}})\|_0\leq C\widetilde{h}.$$

Proof. We have the error equation of temperatures by subtracting (2.13) from (3.3):

$$\bar{a}(\boldsymbol{\theta}-\boldsymbol{\theta}_{\widetilde{h}},\boldsymbol{\omega})+\bar{c}(\boldsymbol{u};\boldsymbol{\theta},\boldsymbol{\omega})-\bar{c}(\boldsymbol{u}_{\widetilde{h}};\boldsymbol{\theta}_{\widetilde{h}},\boldsymbol{\omega})-\bar{a}_\Gamma(\theta_f-\theta_{f,\widetilde{h}},[\boldsymbol{\omega}])+\bar{a}_\gamma(\left[\boldsymbol{\theta}-\boldsymbol{\theta}_{\widetilde{h}}\right],[\boldsymbol{\omega}])=0. \tag{3.15}$$

Taking $\boldsymbol{\omega}=\boldsymbol{\varphi}$ in (3.15) and arranging the terms, we have

$$\begin{aligned}&\kappa_f\|\nabla\varphi_f\|_0^2+\kappa_p\|\nabla\varphi_p\|_0^2+\kappa_f\gamma(\widetilde{h}^{-\frac{1}{2}}\|\varphi_f-\varphi_p\|_\Gamma)^2\\&=-\bar{a}(\boldsymbol{\phi},\boldsymbol{\varphi})-\bar{c}(\boldsymbol{u}-\boldsymbol{u}_{\widetilde{h}};\boldsymbol{\theta},\boldsymbol{\varphi})-\bar{c}(\boldsymbol{u}_{\widetilde{h}};\boldsymbol{\phi},\boldsymbol{\varphi})+\bar{a}_\Gamma(\theta_f-\theta_{f,\widetilde{h}},[\boldsymbol{\varphi}])-\bar{a}_\gamma([\boldsymbol{\phi}],[\boldsymbol{\varphi}]).\end{aligned} \tag{3.16}$$

Now, let us bound each terms on the right-hand side of (3.16) with the help of the Cauchy inequality, Young's inequality, and (3.13).

$$\begin{aligned}|-\bar{a}(\boldsymbol{\phi},\boldsymbol{\varphi})|&\leq\kappa_f\|\nabla\phi_f\|_0\|\nabla\varphi_f\|_0+\kappa_p\|\nabla\phi_p\|_0\|\nabla\varphi_p\|_0\\&\leq\kappa_f\|\nabla\phi_f\|_0^2+\frac{\kappa_f}{4}\|\nabla\varphi_f\|_0^2+\kappa_p\|\nabla\phi_p\|_0^2+\frac{\kappa_p}{4}\|\nabla\varphi_p\|_0^2\\&\leq C\widetilde{h}^2+\frac{\kappa_f}{4}\|\nabla\varphi_f\|_0^2+\frac{\kappa_p}{4}\|\nabla\varphi_p\|_0^2,\end{aligned}$$

$$
\begin{aligned}
&|-\bar{c}(\boldsymbol{u}-\boldsymbol{u}_{\widetilde{h}};\boldsymbol{\theta},\boldsymbol{\varphi})-\bar{c}(\boldsymbol{u}_{\widetilde{h}};\boldsymbol{\phi},\boldsymbol{\varphi})|\\
\leq&\bar{N}\|\nabla(u_f-u_{f,\widetilde{h}})\|_0\|\nabla\theta_f\|_0\|\nabla\varphi_f\|_0+\bar{N}\|u_p-u_{p,\widetilde{h}}\|_0\|\theta_p\|_2\|\nabla\varphi_p\|_0\\
&+\bar{N}\|\nabla u_{f,\widetilde{h}}\|_0\|\nabla\phi_f\|_0\|\nabla\varphi_f\|_0+\bar{N}\|u_{p,\widetilde{h}}\|_0\|\phi_p\|_2\|\nabla\varphi_p\|_0\\
\leq&\bar{N}^2\kappa_f^{-1}\|\nabla(u_f-u_{f,\widetilde{h}})\|_0^2\|\nabla\theta_f\|_0^2+\bar{N}^2\kappa_f^{-1}\|\nabla u_{f,\widetilde{h}}\|_0^2\|\nabla\phi_f\|_0^2+\frac{\kappa_f}{2}\|\nabla\varphi_f\|_0^2\\
&+\bar{N}^2\kappa_p^{-1}\|u_p-u_{p,\widetilde{h}}\|_0^2\|\theta_p\|_2^2+\bar{N}^2\kappa_p^{-1}\|u_{p,\widetilde{h}}\|_0^2\|\phi_p\|_2^2+\frac{\kappa_p}{2}\|\nabla\varphi_p\|_0^2\\
\leq&C\widetilde{h}^2+\bar{N}^2\kappa_f^{-1}\|\nabla\theta_f\|_0^2\|\nabla\psi_f\|_0^2+\frac{\kappa_f}{2}\|\nabla\varphi_f\|_0^2+\bar{N}^2\kappa_p^{-1}\|\theta_p\|_2^2\|\psi_p\|_0^2+\frac{\kappa_p}{2}\|\nabla\varphi_p\|_0^2,\\
&|\bar{a}_\Gamma(\theta_f-\theta_{f,\widetilde{h}},[\boldsymbol{\varphi}])-\bar{a}_\gamma([\boldsymbol{\phi}],[\boldsymbol{\varphi}])|\\
\leq&\kappa_f C_{in}^{\frac{1}{2}}\widetilde{h}^{-\frac{1}{2}}\|\nabla(\theta_f-\theta_{f,\widetilde{h}})\|_0\|\varphi_f-\varphi_p\|_\Gamma+\kappa_f\gamma C_{in}^{\frac{1}{2}}\widetilde{h}^{-\frac{3}{2}}\|\phi_f-\phi_p\|_0\|\varphi_f-\varphi_p\|_\Gamma\\
\leq&\frac{\kappa_f C_{in}}{2\gamma}\|\nabla(\theta_f-\theta_{f,\widetilde{h}})\|_0^2+\frac{\kappa_f\gamma C_{in}}{2}(\widetilde{h}^{-1}\|\phi_f-\phi_p\|_0)^2+\kappa_f\gamma(\widetilde{h}^{-\frac{1}{2}}\|\varphi_f-\varphi_p\|_\Gamma)^2\\
\leq&C\widetilde{h}^2+\frac{\kappa_f C_{in}}{2\gamma}\|\nabla\varphi_f\|_0^2+\kappa_f\gamma(\widetilde{h}^{-\frac{1}{2}}\|\varphi_f-\varphi_p\|_\Gamma)^2.
\end{aligned}
$$

Since $\gamma\gg C_{in}$, the term $\frac{\kappa_f C_{in}}{2\gamma}\|\nabla\varphi_f\|_0^2$ is pretty close to zero. Then bounding the terms as shown above for (3.16) results in

$$
\kappa_f\|\nabla\varphi_f\|_0^2+\kappa_p\|\nabla\varphi_p\|_0^2\leq C\widetilde{h}^2+\varpi_f\|\nabla\psi_f\|_0^2+\varpi_p\|\psi_p\|_0^2, \tag{3.17}
$$

where $\varpi_f=4\bar{N}^2\kappa_f^{-1}\|\nabla\theta_f\|_0^2$, $\varpi_p=4\bar{N}^2\kappa_p^{-1}\|\theta_p\|_2^2$.

Next, we prove the error estimate of velocity. Subtracting (3.1)-(3.2) from (2.11)-(2.12), we arrive at

$$
a(\boldsymbol{u}-\boldsymbol{u}_{\widetilde{h}},\boldsymbol{v})+c_f(u_f;u_f,v_f)-c_f(u_{f,\widetilde{h}};u_{f,\widetilde{h}},v_f)=\nu^2Gr\left((\boldsymbol{\theta}-\boldsymbol{\theta}_{\widetilde{h}})e,\boldsymbol{v}\right). \tag{3.18}
$$

Setting $\boldsymbol{v}=\boldsymbol{\psi}$ in (3.18) and arranging the terms, we obtain

$$
\begin{aligned}
&\nu\|\nabla\psi_f\|_0^2+\frac{\nu}{Da}\|\psi_p\|_0^2\\
=&-a(\boldsymbol{\chi},\boldsymbol{\psi})-c_f\left(u_f;\chi_f,\psi_f\right)_{\Omega_f}-c_f\left(\chi_f;u_{f,\widetilde{h}},\psi_f\right)_{\Omega_f}\\
&-c_f\left(\psi_f;u_{f,\widetilde{h}},\psi_f\right)_{\Omega_f}+Gr\nu^2\left((\boldsymbol{\theta}-\boldsymbol{\theta}_{\widetilde{h}})e,\boldsymbol{\psi}\right).
\end{aligned} \tag{3.19}
$$

To bound the terms on the right-hand side of (3.19), we first consider the nonlinear terms with the help of the Cauchy-Schwarz inequality, Lemma 2.1 and Young's inequality

$$
\begin{aligned}
&|-c_f\left(u_f;\chi_f,\psi_f\right)_{\Omega_f}-c_f\left(\chi_f;u_{f,\widetilde{h}},\psi_f\right)_{\Omega_f}-c_f\left(\psi_f;u_{f,\widetilde{h}},\psi_f\right)_{\Omega_f}|\\
\leq&C\nu^{-1}\|\nabla u_f\|_0^2\|\nabla\chi_f\|_0^2+C\nu^{-1}\|\nabla\chi_f\|_0^2\|\nabla u_{f,\widetilde{h}}\|_0^2+\frac{\nu}{6}\|\nabla\psi_f\|_0^2+N\|\nabla u_{f,\widetilde{h}}\|_0\|\nabla\psi_f\|_0^2\\
\leq&C\widetilde{h}^2+\frac{\nu}{6}\|\nabla\psi_f\|_0^2+N\|\nabla u_{f,\widetilde{h}}\|_0\|\nabla\psi_f\|_0^2.
\end{aligned}
$$

And we have further

$$
\begin{aligned}
&|-a(\boldsymbol{\chi},\boldsymbol{\psi})|\\
\leq&\nu\|\nabla\chi_f\|_0\|\nabla\psi_f\|_0+\frac{\nu}{Da}\|\chi_p\|_0\|\psi\|_0\leq C\widetilde{h}^2+\frac{\nu}{6}\|\nabla\psi_f\|_0^2+\frac{\nu}{4Da}\|\psi_p\|_0^2,\\
&|Gr\nu^2\left((\boldsymbol{\theta}-\boldsymbol{\theta}_{\widetilde{h}})e,\boldsymbol{\psi}\right)|\\
\leq&GrC_p^2\nu^2\|\nabla(\theta_f-\theta_{f,\widetilde{h}})\|_0\|\nabla\psi_f\|_0+GrC_p\nu^2\|\nabla(\theta_p-\theta_{p,\widetilde{h}})\|_0\|\psi_p\|_0\\
\leq&\frac{3Gr^2C_p^4\nu^3}{2}\|\nabla(\theta_f-\theta_{f,\widetilde{h}})\|_0^2+\frac{\nu}{6}\|\nabla\psi_f\|_0^2+Gr^2C_p^2\nu^3Da\|\nabla(\theta_p-\theta_{p,h})\|_0^2+\frac{\nu}{4Da}\|\psi_p\|_0^2\\
\leq&C\widetilde{h}^2+\frac{3Gr^2C_p^4\nu^3}{2}\|\nabla\varphi_f\|_0^2+\frac{\nu}{6}\|\nabla\psi_f\|_0^2+Gr^2C_p^2\nu^3Da\|\nabla\varphi_p\|_0^2+\frac{\nu}{4Da}\|\psi_p\|_0^2.
\end{aligned}
$$

Combining all the terms and according to (3.17) and (3.6), we have the inequality

$$
\begin{aligned}
&\frac{\nu}{2}\|\nabla\psi_f\|_0^2+\frac{\nu}{2Da}\|\psi_p\|_0^2\\
\leq&C\widetilde{h}^2+N\|\nabla u_{f,\widetilde{h}}\|_0\|\nabla\psi_f\|_0^2+\frac{3Gr^2C_p^4\nu^3}{2}\|\nabla\varphi_f\|_0^2+Gr^2C_p^2\nu^3Da\|\nabla\varphi_p\|_0^2\\
\leq&C\widetilde{h}^2+N\nu\xi\eta\|\nabla\psi_f\|_0^2+Gr^2C_p^2\nu^3\max\{\frac{3C_p^2}{2\kappa_f},\frac{Da}{\kappa_p}\}(\kappa_f\|\nabla\varphi_f\|_0^2+\kappa_p\|\nabla\varphi_p\|_0^2)\\
\leq&C\widetilde{h}^2+N\nu\xi\eta\|\nabla\psi_f\|_0^2+Gr^2C_p^2\nu^3\max\{\frac{3C_p^2}{2\kappa_f},\frac{Da}{\kappa_p}\}\varpi_f\|\nabla\psi_f\|_0^2\\
&+Gr^2C_p^2\nu^3\max\{\frac{3C_p^2}{2\kappa_f},\frac{Da}{\kappa_p}\}\varpi_p\|\psi_p\|_0^2.
\end{aligned}
$$

Therefore, if

$$
\begin{aligned}
&\frac{\nu}{2}-N\nu\xi\eta-Gr^2C_p^2\nu^3\max\{\frac{3C_p^2}{2\kappa_f},\frac{Da}{\kappa_p}\}\varpi_f>0,\\
&\frac{\nu}{2Da}-Gr^2C_p^2\nu^3\max\{\frac{3C_p^2}{2\kappa_f},\frac{Da}{\kappa_p}\}\varpi_p>0,
\end{aligned}
\tag{3.20}
$$

then we obtain the following result:

$$
\begin{aligned}
&(\frac{\nu}{2}-N\nu\xi\eta-Gr^2C_p^2\nu^3\max\{\frac{3C_p^2}{2\kappa_f},\frac{Da}{\kappa_p}\}\varpi_f)\|\nabla\psi_f\|_0^2\\
&+(\frac{\nu}{2Da}-Gr^2C_p^2\nu^3\max\{\frac{3C_p^2}{2\kappa_f},\frac{Da}{\kappa_p}\}\varpi_p)\|\psi_p\|_0^2\leq C\widetilde{h}^2.
\end{aligned}
\tag{3.21}
$$

Finally, by using the discrete *inf-sup* condition and results in (3.17), we have

$$
\|\pi_f\|_0\leq C\widetilde{h}+C\|\nabla\psi_f\|_0+C\|\nabla\varphi_f\|_0,\ \|\pi_p\|_0\leq C\widetilde{h}+C\|\psi_p\|_0+C\|\nabla\varphi_p\|_0. \tag{3.22}
$$

The proof ends. □

Now, based on the finite element method (3.1)-(3.3), we give a decoupled two-grid method for solving the stationary closed-loop geothermal model.

Algorithm 1. Decoupled two-grid method.

Step 1. Solve the coupled, nonlinear closed-loop geothermal problem on a coarse grid, i.e., find $(\boldsymbol{u}_H,\boldsymbol{p}_H,\boldsymbol{\theta}_H)\in X_H\times Y_H\times W_H$ by (3.1)-(3.3).

Step 2. Solve the Navier-Stokes/Darcy equations by using a Newton iteration on the fine grid as follows: find $(\boldsymbol{u}^h, \boldsymbol{p}^h) \in X_h \times Y_h$ satisfying

$$\begin{aligned} &a(\boldsymbol{u}^h, \boldsymbol{v}_h) - b(\boldsymbol{v}_h, \boldsymbol{p}^h) + c_f(u_f^h; u_{f,H}, v_{f,h}) + c_f(u_{f,H}; u_f^h, v_{f,h}) \\ &= \nu^2 Gr\,(\boldsymbol{\theta}_H e, \boldsymbol{v}_h) + c_f(u_{f,H}; u_{f,H}, v_{f,h}) \quad \forall \boldsymbol{v}_h \in X_h, \end{aligned} \tag{3.23}$$

$$b(\boldsymbol{u}^h, \boldsymbol{q}_h) = 0 \quad \forall \boldsymbol{q}_h \in Y_h. \tag{3.24}$$

Step 3. Solve a linearized heat problem in the porous media domain Ω_p and fluid domain Ω_f on the fine grid as follows: find $\boldsymbol{\theta}^h \in W^h$ such that for all $\boldsymbol{\omega}_h \in W_h$

$$\bar{a}(\boldsymbol{\theta}^h, \boldsymbol{\omega}_h) + \bar{c}(\boldsymbol{u}^h; \boldsymbol{\theta}^h, \boldsymbol{\omega}_h) - \bar{a}_\Gamma(\theta_f^h, [\boldsymbol{\omega}_h]) + \bar{a}_\gamma(\left[\boldsymbol{\theta}^h\right], [\boldsymbol{\omega}_h]) = (\boldsymbol{g}, \boldsymbol{\omega}_h)\,. \tag{3.25}$$

Then, we show the stability of Algorithm 1.

Theorem 3.3. *Under the assumptions of Theorem 3.1, if the condition $N\xi\eta < 1$ holds, then the solution to Algorithm 1 satisfies the following bounds*

$$\begin{aligned} &(1 - N\xi\eta)\|\nabla u_f^h\|_0^2 + \frac{1}{Da}\|u_p^h\|_0^2 \le \frac{2\nu^2\eta^2(N^2\xi^4\eta^2 + Gr^2C_p^4)}{1 - N\eta\xi} + \nu^2 Gr^2 C_p^2 Da\eta^2, \\ &\|\nabla\theta_f^h\|_0^2 + \|\nabla\theta_p^h\|_0^2 \le \eta^2. \end{aligned}$$

Proof. Setting $\boldsymbol{v}_h = \boldsymbol{u}^h$ in (3.23), we obtain

$$\begin{aligned} \nu\|\nabla u_f^h\|_0^2 + \frac{\nu}{Da}\|u_p^h\|_0^2 =& - c_f(u_f^h; u_{f,H}, u_f^h) + c_f(u_{f,H}; u_{f,H}, u_f^h) \\ &+ \nu^2 Gr\left(\theta_{f,H} e, u_f^h\right) + \nu^2 Gr\left(\theta_{p,H} e, u_p^h\right). \end{aligned} \tag{3.26}$$

Applying Lemma 2.1, Poincaré inequality, and Cauchy-Schwarz inequality, we have

$$\begin{aligned} \nu\|\nabla u_f^h\|_0^2 + \frac{\nu}{Da}\|u_p^h\|_0^2 \le& N\|\nabla u_f^h\|_0^2\|\nabla u_{f,H}\|_0 + N\|\nabla u_{f,H}\|_0^2\|\nabla u_f^h\|_0 \\ &+ \nu^2 GrC_p^2\|\nabla\theta_{f,H}\|_0\|\nabla u_f^h\|_0 + \nu^2 GrC_p\|\nabla\theta_{p,H}\|_0\|u_p^h\|_0. \end{aligned} \tag{3.27}$$

Bound the right-hand side of (3.27) by the Young inequality and Theorem 3.1

$$\begin{aligned} &N\|\nabla u_f^h\|_0^2\|\nabla u_{f,H}\|_0 \le N\|\nabla u_f^h\|_0^2\nu\xi\eta, \\ &N\|\nabla u_{f,H}\|_0^2\|\nabla u_f^h\|_0 \le (\nu - N\nu\xi\eta)^{-1}N^2\nu^4\xi^4\eta^4 + \frac{(\nu - N\nu\xi\eta)}{4}\|\nabla u_f^h\|_0^2, \\ &\nu^2 GrC_p^2\|\nabla\theta_{f,H}\|_0\|\nabla u_f^h\|_0 \le (\nu - N\nu\xi\eta)^{-1}\nu^4 Gr^2C_p^4\eta^2 + \frac{(\nu - N\nu\xi\eta)}{4}\|\nabla u_f^h\|_0^2, \\ &\nu^2 GrC_p\|\nabla\theta_{p,H}\|_0\|u_p^h\|_0 \le \frac{\nu^3 Gr^2C_p^2 Da}{2}\eta^2 + \frac{\nu}{2Da}\|u_p^h\|_0^2. \end{aligned} \tag{3.28}$$

Then, combining (3.28) with (3.27) yields

$$(1 - N\xi\eta)\|\nabla u_f^h\|_0^2 + \frac{1}{Da}\|u_p^h\|_0^2 \le \frac{2N^2\nu^2\xi^4\eta^4}{1 - N\xi\eta} + \frac{2\nu^2 Gr^2C_p^4\eta^2}{1 - N\xi\eta} + \nu^2 Gr^2C_p^2 Da\eta^2. \tag{3.29}$$

Finally, taking $\boldsymbol{\omega}_h = \boldsymbol{\theta}^h$ in (3.25), we derive

$$\left\|\nabla\theta_f^h\right\|_0^2 + \left\|\nabla\theta_p^h\right\|_0^2 \le \eta^2, \tag{3.30}$$

with the condition $\gamma \gg C_{in}$. □

Note that the bound of error between the solution $(\boldsymbol{u}, \boldsymbol{p}, \boldsymbol{\theta})$ to the coupled model (2.11)-(2.13) and the discretization solution $(\boldsymbol{u}^h, \boldsymbol{p}^h, \boldsymbol{\theta}^h)$ to Algorithm 1 is not easy to achieve $O(h + H^2)$ because of the low regularity of the Darcy velocity. In fact, from Theorem 3.2, we just have $\|u_p - u_{p,H}\|_0 \leq CH$. Besides, as Theorem 3.2, one can easily get the error bound of Algorithm 1 which is bounded by $O(h)$.

4. Numerical experiments

This section will present two examples to demonstrate the efficiency of the proposed method in this paper. The first example with an exact solution is provided to test the convergence rates of the finite element solutions. Besides, the second example simulates the heat transfer in a simplified closed-loop geothermal system [21].

4.1. Investigations on exact solution

This example aims to show the relative errors and orders of convergence with the corresponding computational time of Algorithm 1 and the one-grid method (3.1)-(3.3) in the previous section.

Consider the closed-loop geothermal model on the domain $\Omega = [0,1] \times [0,2]$, where $\Omega_p = [0,1] \times [0,1]$, and $\Omega_f = [0,1] \times [1,2]$. Choose $\kappa_f = \kappa_p = 1$, $\nu = 1$, $Da = 1$ and $Gr = 1$. The boundary condition functions and the source terms are chosen such that the exact solution is

$$u_f = \begin{pmatrix} 10x^2(x-1)^2y(y-1)(2y-1) \\ -10x(x-1)(2x-1)y^2(y-1)^2 \end{pmatrix}, \quad p_f = 10(2x-1)(2y-1),$$

$$u_p = \begin{pmatrix} 2\pi \sin^2(\pi x)\sin(\pi y)\cos(\pi y) \\ -2\pi \sin(\pi x)\sin^2(\pi y)\cos(\pi x) \end{pmatrix}, \quad p_p = \cos(\pi x)\cos(\pi y),$$

$$\theta_f = x(1-x)(1-y), \quad \theta_p = x(1-x)\left(y - y^2\right).$$

The finite element spaces we chosen are the well-known MINI element $(P1b-P1)$ for the Navier-Stokes equations in the domain Ω_f, the Raviart-Thomas (RT0) element [19] for the Darcy velocity u_p and the piecewise constant element $(P0)$ for Darcy pressure p_p in the domain Ω_p. Besides, for the temperature in the whole domain Ω, we use the Lagrangian element $(P1)$. In this case, the orders of convergence of flow fluid velocity in H^1 norm, porous media velocity in L^2 norm, pressure in L^2 norm, and temperature in H^1 norm will be 1.

Set the stopping criteria 10^{-6} and the stabilized parameter $\gamma = 10^5$. Choose the coarse mesh size H and the fine mesh size $h = H^2$. We denote the errors $e_{u_{\zeta,h}} = u_{\zeta,h} - u_\zeta$, $e_{\theta_{\zeta,h}} = \theta_{\zeta,h} - \theta_\zeta$, $e_{p_{\zeta,h}} = p_{\zeta,h} - p_\zeta$ and $e_{u_\zeta^h} = u_\zeta^h - u_\zeta$, $e_{\theta_\zeta^h} = \theta_\zeta^h - \theta_\zeta$, $e_{p_\zeta^h} = p_\zeta^h - p_\zeta$, where $\zeta = f$ or p.

The errors of the velocity, pressure, and temperature for the one-grid method and the two-grid method for different values of h are tabulated in Table 1, 2, and 3, respectively. Table 1-3 show that both methods work well and get almost the same relative errors.

Table 1. Comparisons of the one-grid method and two-gird method in velocities.

H^{-1}	h^{-1}	$\|e_{u_{f,h}}\|_0$	order	$\|\nabla e_{u_{f,h}}\|_0$	order	$\|e_{u_{p,h}}\|_0$	order
-	9	9.457e-02	-	2.746	-	4.889e-01	-
-	16	2.992e-02	1.99	1.452	1.10	2.7944e-01	0.97
-	25	1.222e-02	2.00	9.044e-01	1.06	1.796e-01	0.99
-	36	5.884e-03	2.00	6.196e-01	1.03	1.249e-01	0.99
-	49	3.172e-03	2.00	4.518e-01	1.02	9.186e-02	0.99
-	64	1.857e-03	2.00	3.444e-01	1.01	7.035e-02	0.99
H^{-1}	h^{-1}	$\|e_{u_f^h}\|_0$	order	$\|\nabla e_{u_f^h}\|_0$	order	$\|e_{u_p^h}\|_0$	order
3	9	9.465e-02	-	2.748	-	4.889e-01	-
4	16	2.993e-02	2.00	1.453	1.10	2.794e-01	0.97
5	25	1.222e-02	2.00	9.048e-01	1.06	1.796e-01	0.99
6	36	5.887e-03	2.00	6.197e-01	1.03	1.249e-01	0.99
7	49	3.177e-03	2.00	4.519e-01	1.02	9.186e-02	0.99
8	64	1.863e-03	1.99	3.444e-01	1.01	7.035e-02	0.99

Table 2. Comparisons of the one-grid method and two-gird method in pressures.

H^{-1}	h^{-1}	$\|e_{p_{f,h}}\|_0$	order	$\|e_{p_{p,h}}\|_0$	order
-	9	3.907	-	5.831e-02	-
-	16	1.45	1.72	3.277e-02	1.00
-	25	6.545e-01	1.78	2.097e-02	1.00
-	36	3.423e-01	1.77	1.456e-02	1.00
-	49	1.985e-01	1.76	1.069e-02	1.00
-	64	1.245e-01	1.74	8.190e-03	1.00
H^{-1}	h^{-1}	$\|e_{p_f^h}\|_0$	order	$\|e_{p_p^h}\|_0$	order
3	9	3.907	-	5.831e-02	-
4	16	1.45	1.72	3.277e-02	1.00
5	25	6.545e-01	1.78	2.097e-02	1.00
6	36	3.423e-01	1.77	1.456e-02	1.00
7	49	1.985e-01	1.76	1.069e-02	1.00
8	64	1.245e-01	1.74	8.190e-03	1.00

The CPU time for both methods is tabulated in Table 4. As expected, the two-grid method spends less computing time than the one-grid method under nearly the same accuracy.

4.2. Simulation for a closed-loop geothermal system

This example simulates heat transfer in a simplified closed-loop geothermal system, which is studied in [21]. As shown in [21], the computational domain consists of a U-shape heat transfer pipeline and a geothermal reservoir, where the cold fluid is

Table 3. Comparisons of the one-grid method and two-gird method in temperatures.

H^{-1}	h^{-1}	$\|e_{\theta_{f,h}}\|_0$	order	$\|\nabla e_{\theta_{f,h}}\|_0$	order	$\|e_{\theta_{p,h}}\|_0$	order	$\|\nabla e_{\theta_{p,h}}\|_0$	order
-	9	1.492e-03	-	5.227e-02	-	1.146e-03	-	2.686e-02	-
-	16	4.715e-04	2.00	2.944e-02	0.99	3.667e-04	1.98	1.518e-02	0.99
-	25	1.915e-04	2.00	1.885e-02	0.99	1.506e-04	1.99	9.728e-03	0.99
-	36	9.326e-05	1.99	1.309e-02	0.99	7.274e-05	1.99	6.759e-03	0.99
-	49	4.995e-05	1.99	9.619e-03	0.99	3.928e-05	1.99	4.966e-03	0.99
-	64	2.936e-05	1.99	7.365e-03	0.99	2.303e-05	1.99	3.803e-03	0.99
H^{-1}	h^{-1}	$\|e_{\theta_f^h}\|_0$	order	$\|\nabla e_{\theta_f^h}\|_0$	order	$\|e_{\theta_p^h}\|_0$	order	$\|\nabla e_{\theta_p^h}\|_0$	order
3	9	1.489e-03	-	5.227e-02	-	1.145e-03	-	2.686e-02	-
4	16	4.688e-04	2.00	2.944e-02	0.99	3.657e-04	1.98	1.518e-02	0.99
5	25	1.932e-04	1.99	1.885e-02	0.99	1.498e-04	1.99	9.728e-03	0.99
6	36	9.241e-05	1.99	1.309e-02	0.99	7.202e-05	2.00	6.759e-03	0.99
7	49	5.036e-05	1.99	9.619e-03	0.99	3.866e-05	2.01	4.966e-03	0.99
8	64	2.953e-05	1.99	7.365e-03	0.99	2.248e-05	2.02	3.803e-03	0.99

Table 4. Comparisons of the one-grid method with the two-grid method in CPU time.

method	One	Two	One	Two	One	Two	One	Two	One	Two	One	Two
H^{-1}	-	3	-	4	-	5	-	6	-	7	-	8
h^{-1}	9	9	16	16	25	25	36	36	49	49	64	64
CPU time	0.28	0.19	0.89	0.46	2.34	1.03	5.30	2.09	11.29	3.83	22.54	6.94

injected through the left side pipeline, the hot fluid is pumped out from the right side pipeline, and source of heat comes from the geothermal reservoir.

On the left pipeline, the inflow boundary condition is imposed on the top boundary $\partial\Omega_{\text{in}} = \{(x,y)\colon\ y = 4, 0 \leqslant x \leqslant 0.2\}$ with $U_x = 0$ and $U_y = -2048x(0.2-x)$. The boundary condition for temperature is assumed as $\theta_f = 20$. On the right pipeline, the top boundary $\partial\Omega_{\text{out}} = \{(x,y) : y = 4, 3.8 \leqslant x \leqslant 4\}$ is given as the free outflow boundary conditions

$$(-p_f + \nu\nabla u_f)\cdot n_f = 0, \quad n_f \cdot \kappa_f \nabla\theta_f = 0 \quad on \quad \partial\Omega_{\text{out}}.$$

On the other boundaries of the closed-loop pipe $\{(x,y) : x = 0, 1 \leqslant y \leqslant 4\} \subset \partial\Omega_f$, $\{(x,y) : x = 0.2, 1.2 \leqslant y \leqslant 4\} \subset \partial\Omega_f, \{(x,y) : y = 1.2, 0.2 \leqslant x \leqslant 3.8\} \subset \partial\Omega_f$, $\{(x,y) : x = 3.8, 1.2 \leqslant y \leqslant 4\} \subset \partial\Omega_f$, and $\{(x,y) : x = 4, 1 \leqslant y \leqslant 4\} \subset \partial\Omega_f$, we impose the no-slip boundary condition for velocity and the insulated boundary condition for temperature:

$$u_f = 0, \quad n_f \cdot \kappa_f \nabla\theta_f = 0 \quad \text{on } \partial\Omega_f \backslash \Gamma.$$

Besides, on the interface $\Gamma = \{(x,y) : y = 1, 0 \leqslant x \leqslant 4\}$, the interface conditions (2.7)-(2.10), which are proposed for the model, are utilized. The geothermal reservoir domain is $\Omega_p = [0,4] \times [0,1]$. We impose the no-flow boundary condition

$u_p \cdot n_p = 0$ on $\partial\Omega_p \backslash \Gamma$. The homogeneous Neumann boundary condition is considered for the temperature on the left and right walls of Ω_p. At the bottom of the reservoir, we consider a hot wall $\theta_p = 100$.

For the simulation, the parameters are chosen as $\kappa_f = 0.6$, $\kappa_p = 1$, $\nu = 1$, $Da = 10^{-6}$, $Gr = 100$, and $\gamma = 1$. The external body forces g_f, g_p are imposed as zero. Figure 1 shows the temperature distribution for the different Darcy numbers. From this figure, we can see that as the Darcy number increases, the permeability of the porous media increases, and then the porous media flow becomes faster, resulting in increasing heat transfer efficiency from the bottom of Ω_p to the region around the interface. Hence, the geothermal reservoir with a larger Darcy number has better heat transfer.

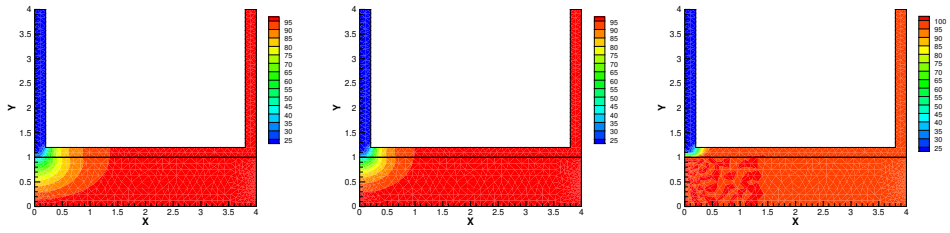

Figure 1. Temperature distribution with different Darcy numbers. Left: $Da = 10^{-6}$; Middle: $Da = 10^{-4}$; Right: $Da = 10^{-2}$.

Next, we investigate and show the effect of different horizontal lengths. From Figure 2, the production temperature is much lower when the horizontal pipeline is shorter due to less heat flux transfer across the interface. This work will help us select the horizontal pipeline length to save construction costs.

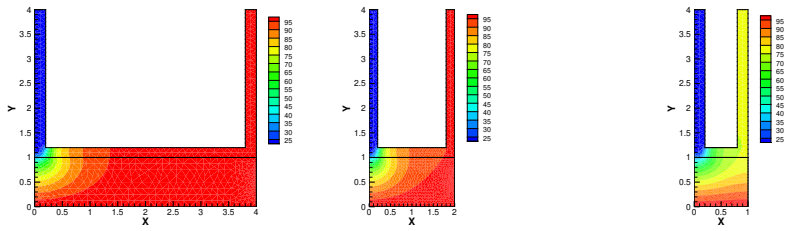

Figure 2. Temperature distribution with different horizontal pipelines. Left: length =4; Middle: length =2; Right: length =1.

In the end, Figure 3 shows the effect of different injection temperatures. As expected, the higher injection temperature provides a higher production temperature on the left pipeline.

Acknowledgements

The authors would like to thank the editor and anonymous reviewers for their helpful comments and suggestions which lead to a considerably improved presentation.

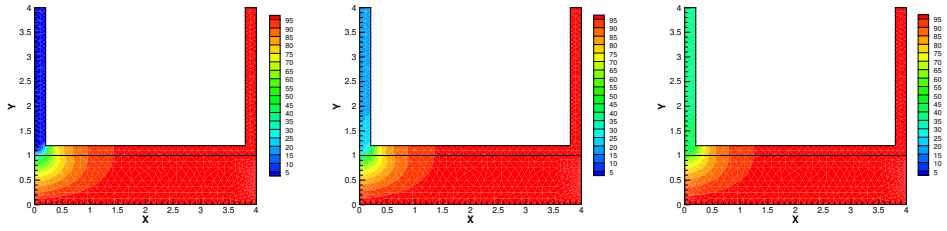

Figure 3. Temperature distribution with different injection temperatures. Left: injection temperature $\theta_f = 0$; Middle: injection temperature $\theta_f = 20$; Right: injection temperature $\theta_f = 40$.

References

[1] R. A. Adams and J. J. F. Fournier, *Sobolev spaces*, Academic Press, New York, 2003.

[2] E. Burman and M. Fernández, *Stabilization of explicit coupling in fluid-structure interaction involving fluid incompressibility*, Comput. Methods Appl. Mech. Engrg., 2009, 198(5–8), 766–784.

[3] G. Du, Q. Li and Y. Zhang, *A two-grid method with backtracking for the mixed Navier–Stokes/Darcy model*, Numer. Meth. Part. Differ. Equs., 2020, 36(6), 1601–1610.

[4] B. Du, H. Su and X. Feng, *Two-level variational multiscale method based on the decoupling approach for the natural convection problem*, Int. Commun. Heat Mass Transf., 2015, 61, 128–139.

[5] J. Fang, P. Huang and Y. Qin, *A two-level finite element method for the steady-state Navier-Stokes/Darcy model*, J. Korean Math. Society, 2020, 57, 915–933.

[6] M. Fernández, J. Gerbeau and S. Smaldone, *Explicit coupling schemes for a fluid-fluid interaction problem arising in hemodynamics*, SIAM J. Sci. Comput., 2014, 36(6), A2557–A2583.

[7] Y. He, Y. Zhang, Y. Shang and H. Xu, *Two-level newton iterative method for the 2D/3D steady Navier-Stokes equations*, Numer. Meth. Part. Differ. Equs., 2012, 28(5), 1620–1642.

[8] X. Hu, P. Huang and X. Feng, *Two-grid method for Burgers' equation by new mixed finite element schemes*, Math. Model. Anal., 2014, 19, 1–17.

[9] P. Huang, *A two-level stabilized Oseen iterative method for stationary conduction-convection equations*, Math. Rep., 2014, 16, 285–293.

[10] P. Huang, *An efficient two-level finite element algorithm for the natural convection equations*, Appl. Numer. Math., 2017, 118, 75–86.

[11] P. Huang and X. Feng, *Error estimates for two-level penalty finite volume method for the stationary Navier-Stokes equations*, Math. Meth. Appl. Sci., 2013, 36, 1918–1928.

[12] P. Huang, X. Feng and Y. He, *Two-level defect-correction Oseen iterative stabilized finite element methods for the stationary Navier-Stokes equations*, Appl. Math. Model., 2013, 37, 728–741.

[13] P. Huang, X. Feng and D. Liu, *Two-level stabilized method based on three corrections for the stationary Navier-Stokes equations*, Appl. Numer. Math., 2012, 62, 988–1001.

[14] P. Huang, X. Feng and D. Liu, *Two-level stabilized method based on Newton iteration for the steady Smagorinsky model*, Nonlinear Anal. Real World Appl., 2013, 14, 1795–1805.

[15] P. Huang, X. Feng and H. Su, *Two-level defect-correction locally stabilized finite element method for the steady Navier-Stokes equations*, Nonlinear Anal. Real World Appl., 2013, 14, 1171–1181.

[16] P. Huang, Y. He and X. Feng, *Two-level stabilized finite element method for Stokes eigenvalue problem*, Appl. Math. Mech. (English Edition), 2012, 33(5), 621–630.

[17] P. Huang, Y. He and X. Feng, *Convergence and stability of two-level penalty mixed finite element method for the stationary Navier-Stokes equations*, Frontiers Math. China, 2013, 8, 837–854.

[18] W. Layton and W. Lenferink, *Two-level Picard and modified Picard methods for the Navier-Stokes equations*, Appl. Math. Comput., 1995, 69(2–3), 263–274.

[19] W. Layton, F. Schieweck and I. Yotov, *Coupling fluid flow with porous media flow*, SIAM J. Numer. Anal., 2002, 40(6), 2195–2218.

[20] H. Liu, P. Huang and Y. He, *Well-posedness and finite element approximation for the steady-state closed-loop geothermal system*, 2022, Submitted.

[21] M. Mahbub, X. He, N. Nasu, C. Qiu, Y. Wang and H. Zheng, *A coupled multiphysics model and a decoupled stabilized finite element method for the closed-loop geothermal system*, SIAM J. Sci. Comput., 2020, 42(4), B951–B982.

[22] M. Mu and J. Xu, *A two-grid method of a mixed Stokes-Darcy model for coupling fluid flow with porous media flow*, SIAM J. Numer. Anal., 2007, 45(5), 1801–1813.

[23] L. Wang, J. Li and P. Huang, *An efficient two-level algorithm for the 2D/3D stationary incompressible magnetohydrodynamics based on the finite element method*, Int. Commun. Heat Mass Transf., 2018, 98, 183–190.

[24] J. Xu, *A novel two-grid method for semilinear elliptic equations*, SIAM J. Sci. Comput., 1994, 15(1), 231–237.

[25] J. Xu, *Two-grid discretization techniques for linear and nonlinear PDEs*, SIAM J. Numer. Anal., 1996, 33(5), 1759–1777.

[26] Y. Zhang, L. Shan and Y. Hou, *Well-posedness and finite element approximation for the convection model in superposed fluid and porous layers*, SIAM J. Numer. Anal., 2020, 58(1), 541–564.

[27] T. Zhang, X. Zhao and P. Huang, *Decoupled two level finite element methods for the steady natural convection problem*, Numer. Algor., 2015, 68(4), 837–866.